

Effects of Lead-Free Solders on Imaging Characteristics of the HP 5DX Laminographic X-ray Inspection System

R. Shane Fazio

Hewlett-Packard Company

As concerns of the environmental impact of lead waste increase, the electronics industry is coming under increasing pressure to reduce or eliminate the use of lead in their manufacturing processes. Circuit assembly providers consequently must develop alternatives to eutectic tin-lead solder for use in their operations. Many ramifications are likely, including an initial decrease in process yield, modifications to process equipment, higher material cost, and an increased need for process control information. The HP 5DX laminographic x-ray inspection system is currently used both to find structural defects in solder joints after reflow and also to provide statistical process control information. However, since the existing HP 5DX is predominantly designed for use with eutectic tin-lead solder compounds, customers purchasing the machine have a valid concern regarding its ability to inspect solder joints constructed with lead-free solders. In this paper we provide a theoretical comparison of x-ray attenuation for various solder compounds. Such a comparison indicates the relative effects of lead-free solders on imaging characteristics in the HP 5DX. To help visualize our theoretical indications, we additionally show both actual and simulated images of joints made with lead-free solder compounds.

1. Introduction

With increasing concern over environmental contamination due to lead waste, the electronics industry is coming under increasing pressure to migrate solder processes away from the usage of eutectic tin-lead solder and towards utilization of lead-free compounds. Such a process change has many ramifications. Foremost will likely be an initial decrease in process yield. An increase in material cost is also likely. When these changes occur, an instrument like the HP 5DX can be invaluable in facilitating development of the new process.

An HP 5DX is useful, however, only if the changes in solder compounds do not have a significant deleterious effect on its imaging characteristics. In fact, current HP 5DX users are already concerned that a process change might render their investment in the system ineffectual.

To help address these concerns, in this paper we provide a theoretical study of some of the effects of lead-free solder on HP 5DX imaging capability. This is done primarily by comparison of x-ray attenuation properties for eutectic tin-lead solder and various lead-free solder compounds. We additionally show both actual and simulated images of solder joints made with different compounds. We find little contrast variation when using lead-free solders, which implies little change in inspectability. Although analysis of false failures on a per application basis is the only true means of characterizing the effects of lead-free solders on HP 5DX performance, this study effectively indicates that the HP 5DX should not experience serious performance degradation when utilized to image joints constructed with lead-free compounds.

2. Basics of X-ray Attenuation

We begin with a discussion of the basics of x-ray attenuation. We introduce the notion of an attenuation coefficient and develop the

model we use for evaluating attenuation in different materials, taking into consideration the HP 5DX energy spectrum. The reader familiar with x-ray attenuation may skip to the next section.

Many factors affect the attenuation of x-rays as they pass through a material. These "factors" are summarized in terms of a number of parameters known as *scattering cross-sections*, which may be loosely thought of as an effective capture area over which an x-ray photon experiences some type of scattering event. X-ray photons experience a variety of scattering interactions, including photoelectric, Compton, pair production, Rayleigh, and photonuclear (Attix [1]). For the energy range in which the HP 5DX operates, photoelec-

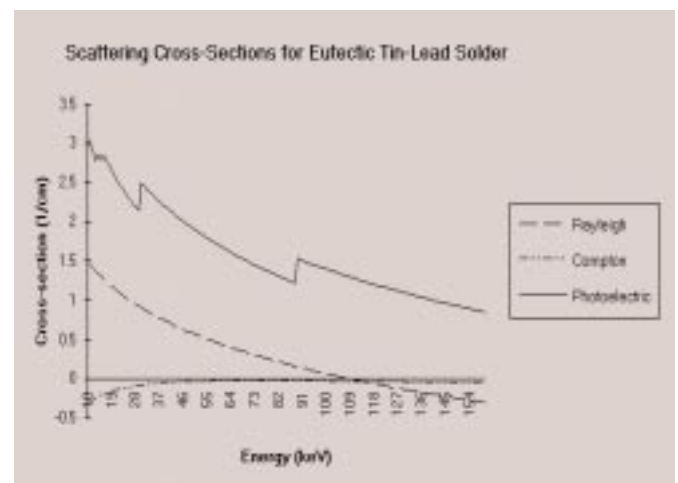


Fig. 1. Scattering cross-sections for eutectic tin-lead solder versus energy. The ordinate is on a \log_{10} scale. Note the dominance of the photoelectric cross-section, followed by the Rayleigh and Compton cross-sections.

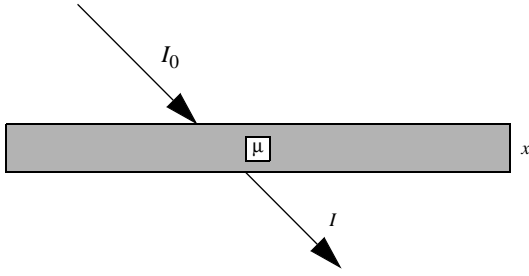


Fig. 2. Illustration of x-ray photons passing through a homogeneous attenuating material of constant thickness

tronic interactions are predominant, followed by Rayleigh and Compton. In Fig. 1 we show these cross-sections as a function of energy for eutectic tin-lead solder. Fortunately, cross-sections may be summed into a single energy dependent parameter that provides all the information necessary to predict bulk attenuation properties. This parameter is known as the *attenuation coefficient*.

Scattering cross sections and attenuation coefficients have been measured for the elements and are readily available (see, e.g., Cullen [4], [5]). Tools such as XOP (Sanchez del Rio and Dejus [15]) can be used with this data to find attenuation coefficients for a wide variety of compounds. Here, we use Harmonex X-ray (Cao and Alvarez [8]), which has built-in attenuation tables, for all our calculations.

Consider a monochromatic x-ray source and any homogeneous attenuating medium of constant thickness x , as shown in Fig. 2. Letting I_0 denote the incident radiation intensity, the transmitted intensity may be written

$$I = I_0 e^{-\mu x}, \quad (1)$$

where μ is the linear attenuation coefficient. Lead, for example, has a linear attenuation coefficient $\mu = 26.43 \text{ cm}^{-1}$ for 80 keV x-rays. (80 keV is the middle of the energy spectrum in the HP 5DX.) Thus, 1 mm of lead reduces transmitted intensity to 7.1% of the incident intensity.

The ability of a material to attenuate the x-rays produced by the HP 5DX depends primarily on three factors: 1) its atomic number, 2) its density, and 3) the frequency of the radiation. Attix [1] shows that the photoelectric cross-section depends on these three factors approximately as

$$\tau \sim \rho \left(\frac{Z}{h\nu} \right)^3 \quad (2)$$

for $h\nu$ below 100 keV, where τ is the photoelectric cross-section, ρ is the density, Z is the atomic number, ν is the radiation frequency, and h is Planck's constant. This expression indicates why lead and other high Z materials are such good attenuators of lower energy x-rays.

Rayleigh scattering behaves as

$$\sigma_R \sim \rho \frac{Z}{(h\nu)^2}, \quad (3)$$

and Compton scales roughly with the density. The attenuation coefficient is obtained by summing the scattering cross-sections.

X-rays are generated by the HP 5DX source by rapidly decelerating high energy electrons. This process leads to radiation known as *bremsstrahlung*. Unfortunately, bremsstrahlung radiation is not monochromatic. We must therefore make a modification to Eq. 1 in order to obtain a more accurate representation of total attenuation. Since the x-ray source is naturally incoherent, we do this by integrating Eq. 1 over the energy spectrum. If we let $p(E)$ denote the fraction of the spectrum with energy E , then we have

$$I = I_0 \int_0^{E_{\max}} e^{-\mu(E)x} p(E) dE. \quad (4)$$

E_{\max} is the maximum energy in the spectrum, which is 160 keV for the HP 5DX.

3. Comparison of Lead-Free Solders with Eutectic Tin-Lead Solder

There are a number of lead-free solder compounds under consideration. We use Eq. 4 to compare attenuations of lead-free solders with eutectic tin-lead solder, which in turn suggests how well the HP 5DX can accommodate these solders. For examples we use some of the solder compounds discussed in Bastecki [2]. In particular, we compare eutectic tin-lead solder (63Sn/37Pb), tin-bismuth (42Sn/58Bi), and a variety of predominantly tin based solders, including tin-silver (98Sn/2Ag), tin-antimony (95Sn/5Sb), tin-indium-silver (77.2Sn/10In/2.8Ag), and tin-silver-copper (96.3Sn/3.2Ag/0.5Cu).

Bastecki classifies solder compounds according to those he deems most likely lead-free alternatives, all of which have at least 95% Sn content. In our analysis we consider three of these (98Sn/2Ag, 95Sn/5Sb, and 96.3Sn/3.2Ag/0.5Cu). The others are provided for comparison purposes.

Eq. 4 must be discretized for evaluation. Using Harmonex ([8]) we compute energy spectra and attenuation coefficients for 16 bands of 10 keV width spanning 10 keV to 160 keV. Eq. 4 in discrete form then becomes

$$I = I_0 \sum_{i=1}^{16} e^{-\mu(E_i)x} p(E_i). \quad (5)$$

The fraction of spectrum at each energy is provided in Fazio [6]. Using this data and accounting for filtration due to the x-ray source anode materials, we obtain values for all $p(E_i)$. The results are summarized in Table 1.*

In Table 2 we provide the *stopping power* (i.e., $1-I/I_0$) for five lead-free solder compounds and eutectic tin-lead solder at thicknesses of 2 mil, 5 mil, 10 mil, and 20 mil. The stopping power indicates the relative amount of x-rays that are attenuated in the material. For example, a stopping power of 0.75 means that three-quarters of the incident radiation is attenuated. Higher numbers consequently imply higher attenuation.

*This spectrum assumes a thin target approximation with a multilayer anode window consisting of 5 μm tungsten, 2 mm beryllium, and 250 μm 304 stainless steel. To account for window filtration, we use the geometry for a 400 FOV.

Table 1. HP 5DX Energy Spectrum

Energy (keV)	$p(E_i)$
10	1.4933×10^{-17}
20	0.0004722
30	0.02795
40	0.07565
50	0.1031
60	0.2176
70	0.1012
80	0.09738
90	0.08965
100	0.07948
110	0.06785
120	0.05524
130	0.04197
140	0.02826
150	0.01424
160	0

Table 2 indicates that 42Sn/58Bi has nearly identical x-ray attenuation as eutectic tin-lead solder. This implies that the imaging characteristics of the HP 5DX for joints made with 42Sn/58Bi will be nearly the same as for 63Sn/37Pb solder. With the other solder compounds, which all consist predominantly of tin, the stopping power is about 88% that of 63Sn/37Pb solder. Images of joints constructed with these compounds will therefore have slightly less contrast.

Ramifications due to reduced contrast depend on both joint thickness and shading. With less contrast shading may be more problematic. On the other hand, thicker joints might be more easily analyzed, since the contrast maps to a more linear portion of the solder thickness calibration curves. Although the HP 5DX is optimized for eutectic tin-lead solder, we believe it should have little difficulty imaging the predominantly tin based solder compounds.*

4. Images

Let's now examine a few images of joints made with alternative solders. In Fig. 3 we show two simulated solder joints. The "joint" on the left consists of eutectic tin-lead solder and has a foreground-

background delta gray level of 50. This level of delta-gray corresponds to roughly 5 mils solder. On the right is shown a "joint" with 88% contrast of that on the left, corresponding to the predominantly tin based solders. The foreground-background delta gray is 44.

Fig. 4 shows an actual HP 5DX image, taken at the 400 FOV, of a set of 20 mil gullwing joints constructed with 63Sn/37Pb solder. In Fig. 5 we show the same image (also taken on an HP 5DX) for joints made with 42Sn/58Bi solder. Note that these two images look almost identical. Indeed, measurement of the foreground gray level in the centers of the heel fillets shows that the attenuations are effectively the same. As discussed previously, this result is not unexpected since the theoretical attenuations so closely match. Fig. 6 is a simulation of how the joints may look if the solder compound is one of the predominantly tin based compounds. There is a slight reduction of contrast.

5. Conclusion

In this paper we demonstrated some effects on HP 5DX imaging characteristics for a few of the current candidates for lead-free solders. A theoretical analysis based upon x-ray attenuation characteristics showed that there is almost no difference between eutectic tin-lead solder and 42Sn/58Bi. We also determined that predominantly Sn based solders lead to a contrast about 88% of that for eutectic tin-lead solder. Consequently, we expect little variation in the inspectability of joints made with these alternative solders. We additionally provided some images of both real and simulated solder joints constructed with these different compounds. These images showed the expected contrast variations.

Although the analysis performed in this paper does not constitute a rigorous proof, it indicates that usage of a number of lead-free solders should not seriously degrade HP 5DX imaging capability. Given that migration to new solder compounds will inevitably lead to a decrease in process yields, and given that the HP 5DX capabilities will most likely not be significantly degraded, the HP 5DX may be a valuable tool to aid the development of processes using lead-free solders.

6. References

- [1] Attix, Frank H. *Introduction to Radiological Physics and Radiation Dosimetry*. John Wiley & Sons: New York, 1986.
- [2] Bastecki, Chris. "A Benchmark Process for the Lead-Free Assembly of

Table 2. Comparison of attenuation of lead-free solders and eutectic tin-lead solder

	Compound	2 mil	5mil	10 mil	20 mil
1	63Sn/37Pb	0.212	0.411	0.608	0.800
2	42Sn/58Bi	0.213	0.414	0.613	0.809
3	98Sn/2Ag	0.188	0.360	0.530	0.703
4	95Sn/5Sb	0.187	0.359	0.529	0.702
5	77.2Sn/10In/2.8Ag	0.187	0.359	0.529	0.702
6	96.3Sn/3.2Ag/0.5Cu	0.187	0.360	0.530	0.702

*The HP 5DX is not designed to work well with conductive epoxies. At this time the industry is not likely to employ conductive epoxy on a large scale. If this situation should change, we will necessarily investigate appropriate inspection techniques.



Fig. 3. Simulated contrast difference between eutectic tin-lead solder and predominantly tin based solders. Tin-lead is on the left and the other, with only 88% of the foreground-background delta gray, is on the right. Delta gray for the tin-lead “joint” is 50, which is typical for about 5 mils solder.

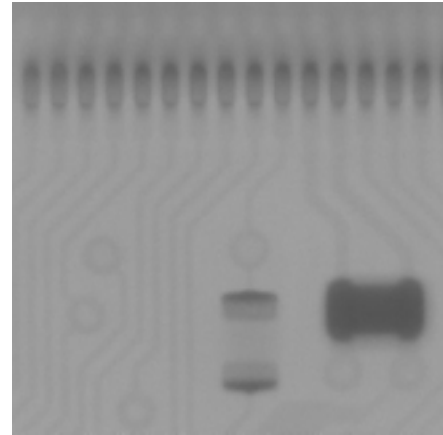


Fig. 6. Simulated image of 20 mil gullwing joints for predominantly Sn based solder.

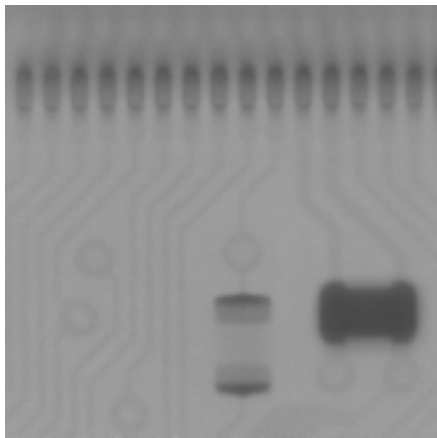


Fig. 4. Image of 20 mil pitch gullwing joints made with 63Sn/37Pb solder. Image was taken at the 400 FOV.

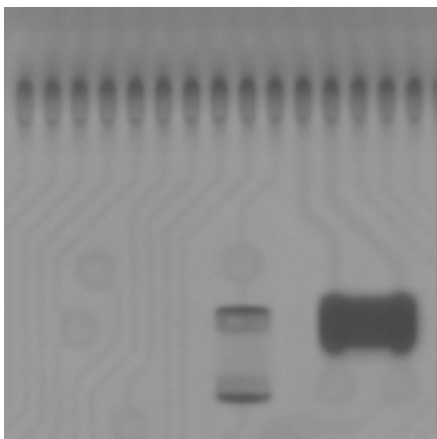


Fig. 5. Image of 20 mil pitch gullwing joints made with 42Sn/58Bi solder. Image was taken at the 400 FOV.

Mixed Technology PCB's,” Technical brief, Alpha Metals Inc., Jan. 1997.

[3] Born, Max and Wolf, Emil. *Principles of Optics*. 6th ed. Pergamon Press: Oxford, 1980.

[4] Cullen, D. E., et. al. “Tables and Graphs of Photon-Interaction Cross Sections Derived from the LLNL Evaluated Photon Data Library (EPDL), Z=1-50.” Lawrence Livermore National Laboratory, Livermore, CA, Vol. 6, Part A, Rev. 4, 1991.

[5] Cullen, D. E., et. al. “Tables and Graphs of Photon-Interaction Cross Sections Derived from the LLNL Evaluated Photon Data Library (EPDL), Z=50-100.” Lawrence Livermore National Laboratory, Livermore, CA, Vol. 6, Part B, Rev. 4, 1991.

[6] Fazio, R. Shane. “Radiation Exposure Levels in the HP 5DX Laminographic X-ray Inspection System.” Hewlett-Packard Company, 1997, preprint.

[7] Gickler, Alan and Willi, Craig. “Contamination of Lead-Free Solders,” *SMT*, Nov. 1997, pp. 44-47.

[8] Harmonex X-ray. Developed by Qizhi Cao and Robert E. Alvarez, 1994. Harmonex Corp, 2369 Laura Lane, Mountain View, CA 94043.

[9] Heitler, W. *The Quantum Theory of Radiation*. Dover Publications: New York, 1984.

[10] Jackson, J. D. *Classical Electrodynamics*. John Wiley & Sons: New York, 1975.

[11] Jacobsen, Chris J. *Techniques and Applications of X-ray Imaging*. Short Course Notes (SC69), SPIE's 42nd Annual Meeting, July 1997.

[12] Mandel, Leonard and Wolf, Emil. *Optical Coherence and Quantum Optics*. Cambridge University Press: Cambridge, 1995.

[13] Michette, A. G. and Buckley, C. J. eds. *X-ray Science and Technology*. IOP Publishing Ltd.: Bristol, 1993.

[14] Pedrotti, Frank L., S. J. and Pedrotti, Leno S. *Introduction to Optics*. 2nd ed. Prentice Hall: New Jersey, 1993.

[15] Sanchez del Rio, M. and Dejus, R. J. “XOP: A Multiplatform Graphical User Interface for Synchrotron Radiation Spectral and Optics Calculations.” European Synchrotron Radiation Facility and Argonne National Laboratory, preprint. (For more information see <ftp://ftpa.aps.anl.gov/pub/xfd/idl/xop/README>, or send email to srio@esrf.fr or dejus@aps.anl.gov)